

Experimental Study on Heat Dissipation in Metallic Foam Filled Heat Sink

Sajida Lafta Ghashim *

Mechanical Engineering Department, College of Engineering, University of Baghdad, Baghdad, Iraq

Received 24 Feb 2024

Accepted 22 Jun 2024

Abstract

The need for high speed and reduction in size in electronic components leads to a rise in the power dissipation needed for thermal management. In this research, experiments have been carried out to examine the thermal efficiency from heat sink located on an energy source in a channel. A total of 4 test models with different shapes were tested. Model 1 conventional heat sinks is made from aluminum, model 2 fin heat sinks is made from metal foam, model 3 plate heat sink is made from metal foam and model 4 fin heat sinks filled space between the fins with metal foam; all models have the same flat plate surface area. Copper metal foam of constant pore density of 40 PPI and constant porosity of 0.91 were used. The test runs are done at the air flow rates ranging between (1.2 to 3.3) m/s with the inlet air temperature is 27 °C. The outcomes revealed that the model 3 heat sinks have a greater heat transfer coefficient and a lower thermal resistance than the other types of heatsinks. At input velocity of 3.3 m/s and high power of 30 W, model 3 has the best Nusselt number ratio it has increased from models 2 and 4 by 13.7% and 6.8%, respectively. The plate foam heat sink model 3 has a larger pressure drop when compared to conventional fin heat sink model 1. Moreover, the pressure drop between Models 2 and Model 4 is not significantly different. Additionally, at higher flow rates, the model 3 heat sinks show a 22% reduction in thermal resistance compared to the model 1 at a power of 30 W.

© 2024 Jordan Journal of Mechanical and Industrial Engineering. All rights reserved

Keywords: Nusselt number, metal foam, fins, heat transfer, thermal resistance.

Nomenclature

| | |
|-----------------|--|
| A | area, m ² |
| C _f | inertial coefficient |
| C _p | specific heat capacity at a constant pressure, J/kg·°C |
| D _h | hydraulic diameter, m |
| f | friction factor |
| h | heat transfer coefficient, W/m ² ·°C |
| K | permeability of the metal foam, m ² |
| Nu | Nusselt number |
| n | number of fin |
| P | pressure, Pa |
| P _o | electrical power, W |
| PPI | pore per inch |
| Q | rate of heat transfer, W |
| Re | Reynolds number |
| R _{th} | thermal resistance, °C/ W |
| T | temperature, °C |
| u | velocity, m/s |
| V | voltage, Volt |

Greek symbols

| | |
|---|------------------------------|
| μ | dynamic viscosity, kg/m·s |
| ρ | density, kg/m ³ |
| λ | Thermal conductivity, W/m·°C |
| β | porosity |

Subscripts

| | |
|-----|---------|
| in | inlet |
| out | outlet |
| ave | average |
| w | wall |

1. Introduction

The rapid advancement of higher-density semiconductor packaging for efficiency has caused integrated circuits to generate excessive heat. For this reason, efficient heat removal has been required in order for difficult electronics to operate continuously [1]. Using expanded heat transfer surfaces and raising the cooling flow rate are two ways to improve thermal heat transfer. Fin heat sinks are usually used to provide the extended heat transfer surfaces. Thus, many researches have been done on fin heat sink

* Corresponding author e-mail: sajda_lafta@yahoo.com.

optimization and forced convection design [2]. In an attempt to improve heat dissipation, more research has been done on a variety of fin heat sink designs, including pin-fin, skive-fin, strip-fin, and others [3] [4] [5] [6] [7] [8]. [9] examined experimentally and numerically the thermal efficiency of several types of heat sinks. Heat flux ranges from (3954 to 38357) W/m^2 and Reynolds number between 23597 and 3848.9 are used in the experiments. Air is the working fluid utilized. There are six types of plate heat sinks which are examined in a wind tunnel: curved, zigzag, flat, cross-cutting, and perforated. For three-dimensional flow and forced convection numerical simulations using the FLUENT 15 program, it is combined with a momentum and energy equations with a $(k-\epsilon)$ model of turbulence. According to the outcomes, the system's thermal performance is significantly impacted by the Reynolds number. As the speed of the free stream rises, the heat transfer coefficient also rises, leading to a decrease in the thermal resistance. Additionally, the dependence of thermal resistance and the coefficient of heat transfer on heat flux was discovered. According to a comparative study of several heat sink designs, the perforated cut heat sink had the lowest thermal resistance, the highest Nusselt number, and the best thermal performance. [10] investigated experimentally the performance of heat dissipation from V-corrugated aluminum fin heat sink. An aluminum cylinder of 40 cm in length and 6 cm in diameter was used as the heat sink. Surrounding the heat sink, six aluminum V-corrugated fins were mounted vertically and equally spaced. The fins measured 25 by 25 cm and had a thickness of 2 mm. There were twenty seven holes with 1 cm was made. There are two designs for the holes: staggered and inline. The results demonstrated that V-corrugated fins disperse heat better than flat plate. Additionally, the inline perforated fin provided an enhancement percentage of 36% higher than the solid one. Also, a higher enhancement percentage of 45% was obtained with a staggered perforation procedure. [11] studied experimentally and numerically analyze the thermal performance of three different shapes of fin plate (smooth, perforated, and dimple) heat sinks with two kinds of nanofluids of Al_2O_3 – water and CuO-water. Numerical simulations using the FLUENT 15 program are combined with a momentum and energy equations with a $(k-\epsilon)$ model of turbulence. The study showed that using of nanofluids provided higher average performance and Nusselt number in comparison to traditional liquid cooling. In comparison with the other type of plate fin configuration used in this investigation, the perforated fin plate demonstrated more air heat dissipation. Numerical results that supplied a good confirmation of heat transfer enhancement in the studied ranges validated the experimental results. [12] studied numerically thermal efficiency of heat sinks with perforated fins exposed to a fixed heat flux $4340 W/m^2$. A single piezoelectric fan with various amplitudes (25, 30, and 40) mm placed eccentrically at the duct entrance. Ansys17.2 was used to solve and analyze the numerical. For two kinds of circular axial and lateral perforations, the patterns of air flow and distribution of temperature is explained by a numerical solution. At the highest fan amplitude, the results showed an increase in the heat transfer rate of roughly 12% in axial perforation and 25% in lateral perforation. [13] experimentally investigated flat plate fin heat sinks with discontinuous heating with

forced convection flow. The impacts of the heating size, heating place, and rate of flow on the thermal performance and base temperature profile were examined. As a result, it was demonstrated that, compared to heat sinks under turbulent flow, the ideal heating place for heat sinks under laminar developing flow was on the upstream side. [14] examined the heat transfer from rectangular fins on a horizontal plane using computational and experimental methods at Reynolds number between 2600 and 6800. In a wind tunnel, heat input and inlet air speed were varied but maintained a specific fin number, fin spacing, and fin length. To clarify additional important elements of heat transmission and fluid flow, three-dimensional heat transmission simulations were conducted. The experimental findings demonstrated that the Nusselt number and Reynolds number exhibit an approximately linear relationship in forced convection heat transfer. This relationship also exhibited a reasonable degree of agreement with the existing empirical correlations for fully developed turbulent convective flow for tubes with a fixed heat flux. It is demonstrated that the amount of heat transferred per channel increases with channel length in a straight line but remain about constant when the total number of fins increases. [15] conducted experimentally the heat transmission from vertical cylinders with split pin fins by natural convection. Studies have been performed to find out the rates of heat transmission from finned cylinders to ambient air at different cylinder surface temperatures, angles of fin pitch, and fin heights. The results of the experiments indicate that compared to normal vertical cylinders with plate fins, vertical cylinders with split pin fins exhibit a 20% lower heat resistance. Additionally, the estimated thermal resistance values provide a correlation for the Nusselt number. Heat transmission from both oblique and straight fin heat sinks were experiments carried out by [16]. In this experiment, the heat dissipation characteristics of fin heat sinks manufactured from metal insert filament (brass and bronze) and carbon-based filament (Ice9 Flex) under conditions of forced convection with the Reynolds number of $(7.45 \times 10^4$ to $3.60 \times 10^5)$. Compared to straight fins, oblique fins were found to more efficiently decrease heat sinks' thermal resistance, improve thermal heat transmission, and increase inner-fin velocity, all of which led to a lower pressure loss. It was demonstrated that the carbon-filled polymer (Ice9 Flex) heat sink could dissipate heat significantly more effectively than metal-filled filament heat sinks. [17] examined experimental the forced convection flow from several types of heat sink designs. An experiment was carried out to compare of 12 types of heat sinks, comprising 3 kinds of fin-pin heat sinks with rectangular pins, 3 kinds of fin-pin heat sinks with circular pins, 3 kinds of fin-pin heat sinks with conical pins, and 3 types of simple fin heat sinks in 5, 7, and 9 fin types. The findings demonstrated that, when heat sinks with the same number of fins were compared, heat sinks with conical fins on the 7 and 9 fin types had a higher coefficient of heat transfer and less thermal resistance than other designs of heat sinks with the similar number of fins; the conical fins had a greater convection heat transfer coefficient than the plate fin heat sink. In addition, the plate-fin heat sink in the 5 pin fin heat sink design had the least quantity of heat transmission because of its larger surface area in relation to the flowing air current. Numerous investigations examining

porous heat sinks and utilizing metal foams showed a significant improvement in heat transfer [18] [19] [20] [21] [22] [23]. The use of porous structures was encouraged since they naturally provide a large area for heat transmission between cool air and solid surfaces. Heat sink designed from open-cell metal foams, have a significantly larger porosity, which allows for greater permeability and lighter weights than those traditional heat sinks. Because of these important advantages, metal foams are becoming more and more useful for LED cooling in domestic and automotive applications [24]. The characteristics of heat transmission from an aluminum foam heat sink positioned over a source of heat in a channel have been studied through experiments by [25]. Pore density of aluminum foam heat sinks and Reynolds number vary between the following ranges: (10, 20, and 40) pores per inch and (710 to 2900), respectively. Using an aluminum foam heat sink with low pore density is found to significantly minimize thermal resistance because of the heat sink's very high airflow. [24] examined experimentally the natural convection from metal foam heat sinks with open slots. The sample that was tested was manufactured in-house by connecting multiple foam segments that were fixed to have a length of 100 mm and a width of 10 mm. A total of 29 test samples was examined in both horizontal and vertical directions for every sample, with varying slot widths (0, 2.86, 5, 8, 12.5, and 20) mm and the foam heights (10, 20, 40, 60, and 80) mm. According to experimental results, for a specific heat sink volume, there is an optimal open slot width of (5 to 8) mm for the greatest heat transfer coefficient. When compared to a single foam block ($s = 0$ mm), the coefficient of heat transfer has increased by (14.9, 21.3, 37.6 and 38.2) % at the foam height of (10, 20, 40, and 80) mm, respectively. [26] investigated numerically the heat transmission from pin fin heat sinks made from metal foam and compared with traditional solid pin fin heat sinks. Utilizing aluminum metallic foam with 10 pores per inch and the porosity of 0.93. The finite volume approach is used to discretize the three-dimensional flow by using equations of continuity, momentum, and energy equations in order to study the features of the friction factor and turbulent flow in the metal foam pin fin heat sink. The number of pins, the height ratio of the pins, and the pin diameter ratio were examined. Throughout the whole investigation, the total pin volume stays constant. The findings demonstrate that when compared to solid pin fin heat sinks, the metallic foam heat sinks perform significantly in terms of heat dissipation and friction loss reduction. [27] carried out a numerical analysis to evaluate the cooling characteristics of heat sinks based on PCM integrated with aluminum foam. While maintaining the heat flux kept fixed at 3200 W/m^2 , the efficiency of the PCM- heat sink is examined under a range of operating conditions, such as porosity of metal foam (100, 97, and 90)%, two types of PCM (RT35HC and RT44HC), and three various coefficient of heat transmission amounts (10, 20, and 30) $\text{W/m}^2 \cdot ^\circ\text{C}$. The findings demonstrate that, when comparing the RT35HC-filled heat sink to the RT44HC-based heat sink, the first demonstrated superior cooling capabilities. In comparison to the no-metal foam case, the addition of aluminum foam reduced the base temperature by nearly (6 and 5) $^\circ\text{C}$ for the porosity (97% and 90%) accordingly. Additionally, an additional reduction in the base temperature by nearly (5 and 4) $^\circ\text{C}$ was found in the

porosity (97 and 90) % cases in the RT44HC based heat sink. The heat transfer coefficient increased, resulting in an increased melting time for PCM.

From a review of the literatures mentioned above, little research has been studying the effects of metal foam thickness in heat sinks. Therefore, the purpose of this research is to design four models configuration of heat sinks has the same flat plate surface area and comparisons between the models and find the best model give a high thermal performance with low pressure loss. Additionally, study how will the metal foam effect on thermal resistance in heat sink.

2. Experimental apparatus and procedure

2.1. Fins design

In this study, aluminum fins have been examined and used as conventional heat sinks. The conventional heat sink (model 1) consists of 7 fins were constructed from aluminum alloy 6063 -T5 with thermal conductivity $167 \text{ W/m} \cdot ^\circ\text{C}$, and emissivity 0.8. The sizes of the fin array under investigation are: $L = 80 \text{ mm}$, $H = 20 \text{ mm}$, $s = 3 \text{ mm}$, and $t = 2 \text{ mm}$ as shown in **Fig.1**. Four models were used to perform the experiments as seen in **Fig.2**; model 1 conventional heat sinks made from aluminum, with number of fin 7 of thickness 2 mm, model 2 heat sinks made from metal foam with number of fin 4 of thickness 10 mm, model 3 block foam heat sink and model 4 fin metal foam with number of fin 3 of thickness 10 mm and aluminum fin with number of fin 4 of thickness 5 mm, all models have the same flat plate surface area ($50 \times 80 \times 2$) mm. The current experiment involves the use of a 40 PPI copper metal foam sheet. Imported copper foam comes in the shape of (50×50) cm^2 sheets with a thickness of 10 mm, supplied from Beijing Composite Materials Co., Ltd. in China. Using a water jet CNC machine, the metal foam sheet was cut into sections. To avoid any spaces between the metal foam and plate surface, the specimen's outer surround was designed with accuracy.

2.2. Experimental set up

The evaluations of heat transmission from horizontal surfaces with rectangular fins were carried out in a wind tunnel, which is shown in **Fig.3** and **Fig.4**. The experimental design of the wind tunnel consists of filtration system, nozzle, test section, a diffuser, and a centrifugal fan. The fan is located inside the channel that delivers air to the test section. A flow regulator (screen) with honeycombs at the air inlet side of the wind tunnel is used to break up huge eddies that may occasionally enter the working area and to reduce the air stream's swirling motion. An electric motor with variable speed drives a fan on the tunnel's side to create the airflow. A strainer at the tunnel's base directs air into the working area, where it passes through a contraction cone. The test section consists of a rectangular channel with dimensions of ($340 \times 340 \times 600$) mm as shown in **Fig.5**. A heat sink placed in the test section of the wind tunnel, with an electrical heating element mounted to the bottom of the heat sink with power supply range of (14 to 40 W). To regulate the power input, voltage regulator type (TDGC2-2/0.5), maximum output current 8Am, rating capacity

2KVA , input voltage 220 V , and output voltage (0 to 250) V is attached to the power supply. Digital clamp multi-meter (type KT55 , range 200 Am , resolution 100 mA and accuracy of 2%) is employed to determine the current flowing through the heater. Thermocouples k-type with a specified accuracy of $\pm 0.5\text{ }^{\circ}\text{C}$ are used to measure the temperature . 9 thermocouples were utilized to measure the surface temperatures of the plate fin as well as the air temperatures at the entrance and downstream of the test region. Every thermocouple was calibrated. A digital thermometer (12 stations with storage card, scheme: BTM - 4208SD, Lutron the company, Taiwan) is used to measure the temperature. To reduce the thermal contact resistance between the heat sink plate and the electrical heater sheet, thermal material with thermal conductivity $0.7\text{ W/m}\cdot^{\circ}\text{C}$ was carefully applied to the contact surfaces. Reynolds number ranges from 2700 to 12000, which is considered to be in the turbulent flow. Additionally, two pressure taps, one upstream and one downstream of the fin heat sink, were used to measure the pressure drop across the heat sinks. The taps are connected to two piezometers. The size of piezometers is 1cm diameter and 1.5m length.

2.3. Experiment procedure

To carry out the experiment, every component of the apparatus is attached and checked. The instrument is then

operated, and the required air velocity is adjusted. For maintaining a constant heat flux for heat sinks, an electrical heater was employed. A digital clamp multi-meter is used to measure the current passing through the heater, and a voltage regulator is utilized for setting the power supplied to the heater at a specific value. The hot wire anemometer is mounted to measure the velocity of the airflow. When each heat sink test is finished and the system has reached thermal stability. After that, it is measuring every temperature at different points on the heat sink. Repeat the test with all heat sink models at five different fluid velocities (1.2 to 3.3) m/s and ratings of power (14 to 30) W.

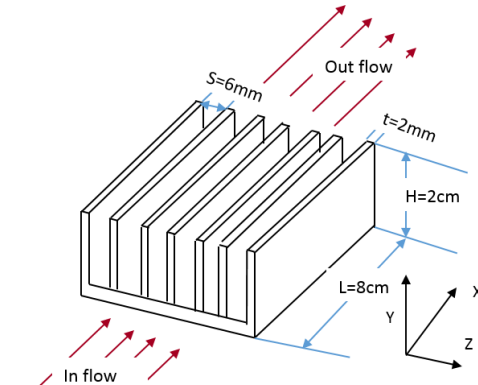


Figure 1. Diagram of the configuration of the fin heat sink

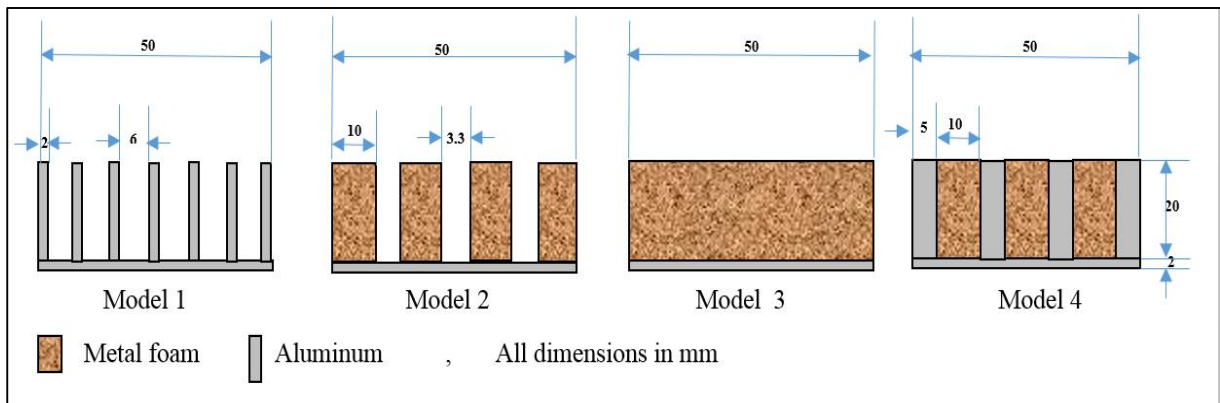


Figure 2. Models of heat sink types



1.Centrifugal fan 2.Conical section 3. Calming section 4.Test section 5. Honey combs
6.Measurements (Thermocouples , Watt meter) 7. Pressure gauge

Figure 3. Picture of an experimental apparatus

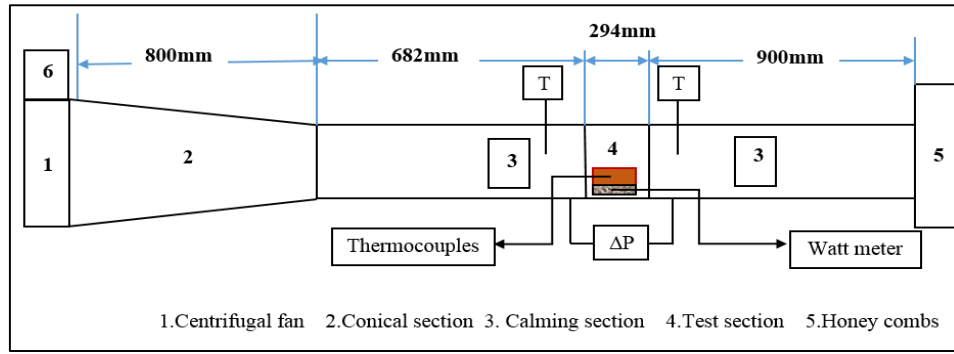


Figure 4. Schematic of an experimental apparatus

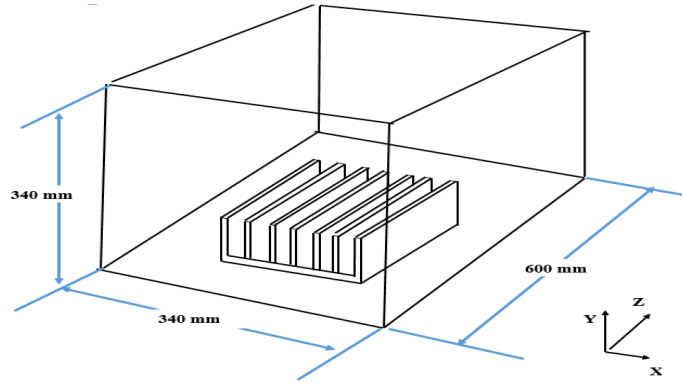


Figure 5. Schematic of the computational domain

3. Data calculations

In this investigation, the following parameters were computed:

The hydraulic diameter of fin channel can be expressed as[14]:

$$D_h = 4 \frac{A}{P} \tag{1}$$

Where:

$P=2+SH$:is the wetted circumference of the fin channel
 $A=SH$: is the cross-sectional area.

The corresponding Reynolds number is[28] :

$$Re = \frac{\rho u_{in} D_h}{\mu} \tag{2}$$

Where the air properties were taken at average air mean temperature (T_f) [29].

$$\rho = 362.74 * (T_f)^{-1.004} \tag{3}$$

$$\mu = 4.112 * 10^{-6} + 5.052 * 10^{-8} * T_f - 1.434 * 10^{-11} * (T_f)^2 + 2.591 * 10^{-15} * (T_f)^3 \tag{4}$$

$$C_p = 1061.332 - 0.4328 * T_f + 1.02344 * 10^{-3} * (T_f)^2 + 6.474 * 10^{-7} * (T_f)^3 + 1.386 * 10^{-10} * (T_f)^4 \tag{5}$$

$$\lambda = -7.488 * 10^{-3} + 1.708 * 10^{-4} * T_f - 23.757 * 10^{-6} * (T_f)^2 + 220.117 * 10^{-12} * (T_f)^3 - 945.995 * 10^{-16} * (T_f)^4 + 1579.57 * 10^{-20} * (T_f)^5 \tag{6}$$

Where :

$$T_f = \frac{T_{in}+T_{out}}{2} \tag{7}$$

The heat transfer coefficient [30] and Nusselt number [31] are estimated as follows :

$$h = \frac{Q}{A (T_{w,ave} - T_f)} \tag{8}$$

$$Nu = \frac{h D_h}{\lambda} \tag{9}$$

Where $T_{w,ave}$ and T_f , the average heated wall temperature and the surrounding air temperature, respectively.

The electrical heat input to the heating element is [32]:

$$Po = V.I \tag{10}$$

The heat transfer from the heated wall:

$$Q = Po \tag{11}$$

The coefficient of friction, expressed as[33]:

$$f = \frac{2 \Delta P D_h}{L \rho u_{in}^2} \tag{12}$$

The definition of thermal resistance is as follows [34]:

$$R_{th} = \frac{\Delta T}{Q} = \frac{(T_{w,ave} - T_f)}{Q} \tag{13}$$

Where $\Delta T = T_{w,ave} - T_f$ is temperature difference .

4. Parameters of metal foam

To examine pore density (PPI), the FEI inspect S50 scanning electron microscopy (SEM) instrument is displayed in Fig.6. It is used to accurately explain the sizes of the pores and ligaments. To determine the PPI of the porous copper foam, some photos were taken shown in Fig.7 . Tests are taken in the Department of Materials Engineering, University of Technology/ Iraq. To calculate the examined pores per inch PPI, the following equation is used :

$$\frac{(dp)_{ave} + (dlig)_{ave}}{\text{lenght of sample per inch}} = PPI \tag{14}$$

The density and porosity of copper metal foam are estimated as follows [35]:

$$\rho_{cal} = \frac{\text{Mass}}{\text{Volume}} \tag{15}$$

$$\beta = 1 - \frac{\rho_{cal}}{\rho_{th}} * 100\% \tag{16}$$

Where

Mass : weight of copper metal foam (kg)

Volume : Sample of metal foam (m³) (Length × Width × Height)

ρ_{th} = theoretical density of copper 8933 kg/m³ [36]

To evaluate the permeability (K) and inertial coefficient (C_f) using the Forchheimer extended Darcy's formula [37]:

$$\frac{\Delta P}{L} = \underbrace{\frac{\mu}{K} u}_{\text{Darcy term}} + \underbrace{\frac{\rho C}{\sqrt{K}} u^2}_{\text{Forchheimer term}} \tag{17}$$

The values for permeability and inertial coefficient were calculated by fitting the pressure loss of measured metal foam according to the above equation (17). Experimental measurements revealed the properties of metal foam used in the study: density 909.575 kg/m³, porosity of 0.91, inertial coefficient 0.119 and the permeability of $1.88 \times 10^{-8} \text{ m}^2$.

5. Uncertainty analysis

The primary sources of uncertainty in this experiment are mistakes in the power, thermocouple, and physical dimension measurements. The uncertainty in parameters

was obtained using the equation analysis prescribed by [38] [39]:

$$\delta R = \frac{\partial R}{\partial x_1} \delta x_1 + \frac{\partial R}{\partial x_2} \delta x_2 + \dots + \frac{\partial R}{\partial x_n} \delta x_n \tag{18}$$

$$W_R = \left[\left(\frac{\partial R}{\partial x_1} W_1 \right)^2 + \left(\frac{\partial R}{\partial x_2} W_2 \right)^2 + \dots + \left(\frac{\partial R}{\partial x_n} W_n \right)^2 \right]^{1/2} \tag{19}$$

The accuracy of the measurement of the variables length, voltage and current had respective errors of ± 0.0005 m, ±0.01 V and ±0.01A. The accuracy of thermocouple ± 0.05 °C. Generally, an error can be classified as systematic or random based on whether it is constant or varies throughout the duration of a single experiment. The maximum uncertainty of the friction factor 10 %, Reynolds number 0.87 %, and Nusselt number 3.8 %.

6. Validation of the computational model

The experimental outcomes for the traditional fin heat sink (model 1) are compared with the results from [14] in Fig.8. In the current study, the numbers of fin 7 and power 14 W, with a range of Re number from 2700 to 12000, in contrast the data in [14] number of fin 6 and power 13.4 W, and range of Re number from 2800 to 6800. At Re number less than 5800, the maximum relative error is approximately 3%, and it decreases to 0.5% at Re number of 7000, demonstrating an acceptable degree of agreement between the two results.



Figure 6. The FEI inspect S50 scanning electron microscopy (SEM) instrument

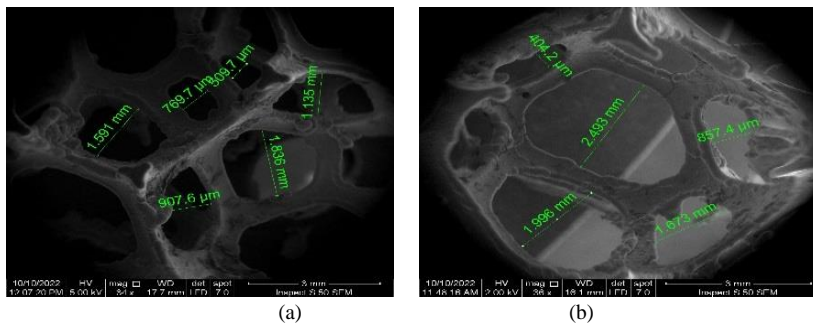


Figure 7. The images of SEM of pores diameter for 40 PPI.

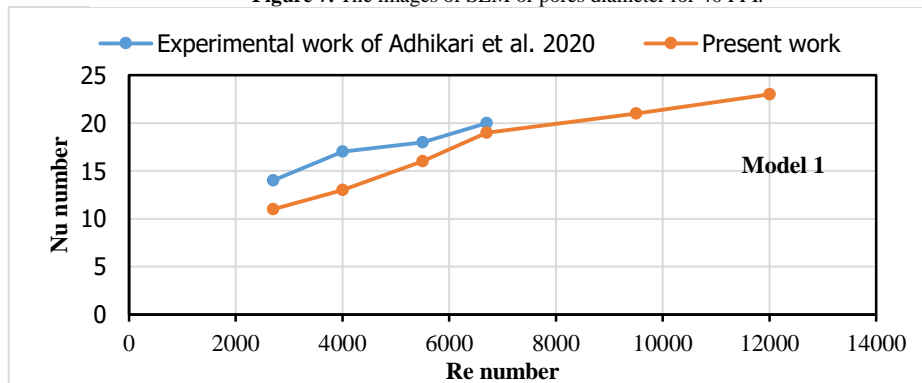


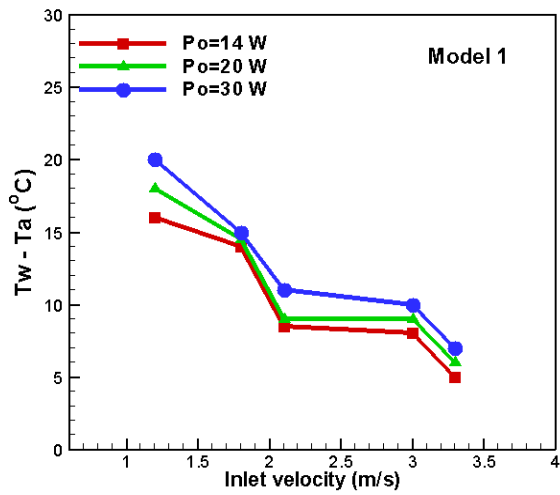
Figure 8. Nusselt number verse Reynolds number

7. Results and discussion

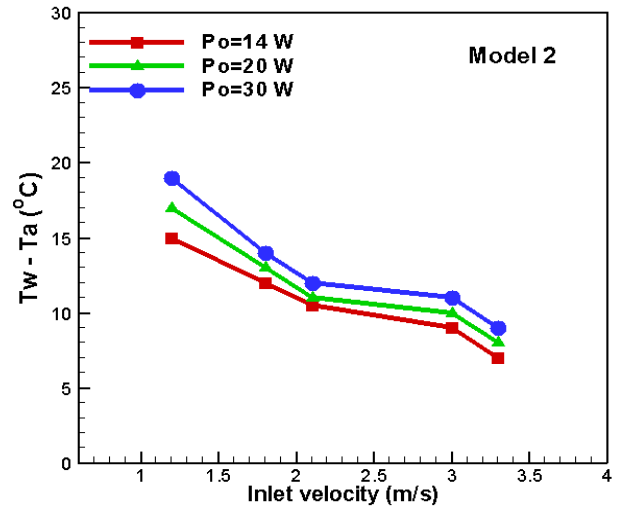
An experimental study on forced convection flow in horizontal channel, without and with metallic foam heat sink , with lower wall heated at uniform heat flux form (14 to 30) W . A comparison between the four models configurations was performed , studied the presence of the foam and determined a better thermal heat transfer with respect to the conventional model (model 1) .

Fig.9 presents the temperature difference ($T_w - T_a$) distributions with inlet velocity for different models under

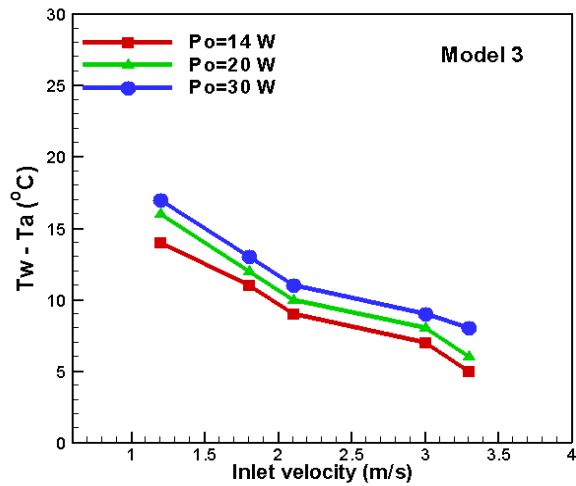
several typical electric power in the range of (14-30) W. The findings show that, while the heat flux remains constant, the improved convective heat transfer caused the temperature distribution to decrease as the inlet velocity increases. The distribution of local temperatures decreases and reaches its smallest value when the velocity is high. Compared to the various models , the model 3 temperature distribution demonstrates clearly reduction. Because the foam provides a greater convective heat transfer area, it shows the heat transfer augmentation obtained by utilizing 40 PPI was significant under the conditions studied.



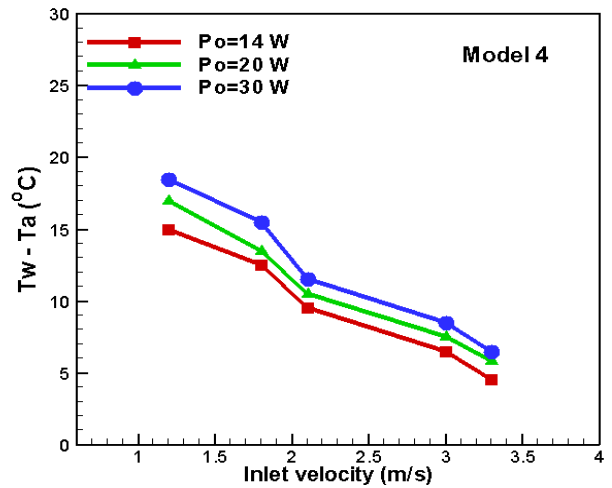
(a) Model 1



(b) Model 2



(c) Model 3



(d) Model 4

Figure 9. Variation of the temperature difference with inlet velocity

The average Nusselt number of the various models of fin heat sinks with inlet velocity of air is displayed with different value of heat flux in **Fig.10**. It is demonstrated that the level of the average Nusselt number substantially increases with the increase of velocity of air, particularly for the heat sink made from metal foam (model 3) or with insert metal foam (model 4). It is evident that the a significant value of Nusselt number improvement is noticed at the higher values of inlet velocity. Additionally, it's discovered that the increase rates of Nu number for metal foam heat sinks model 2 and model 4 are extremely similar and are almost linear with small values different. The model 3 heat sink exhibits(16–27) % greater results than model 1 in the range of air flow rates ranging between (1.2 to 3.3) m/s at electric power 14 W. It is essential to note that the model 3 which is filled fully with metallic foam this lead to increase surface area and this occurrence is developed reduced airflow through a porous medium which has higher pore density, high flow resist. The Nu number of a heat sink filled with or made of metallic foam with high thermal conductivity increases significantly and exceeds the level of Nu number for the conventional heat sinks made from aluminum. The result indicates that the rate of convective

heat transfer efficiency of fin heat sink is significantly influenced by the rate of mass flow and the configuration of the heat sink. Also, the average Nu number of model 3 enhancement from model 1 by (33, 37, and 53)% in power (14, 22, and 30) W was observed at higher flow rate of 3.3 m/s.

With the goal to investigate the impact of heat sink configurations on hydraulic performance, the pressure loss of the fin heat sink was chosen for examination. For the value of inlet velocity examined, it was demonstrated that the models of heat sink have higher influence on the pressure loss, therefore, **Fig. 11** displays the outcomes for different models. It is observed that for all kinds of fin heat sink models, the friction factor along the fin heat sinks decreases greatly with an increase in the inlet velocity. This is because increased air velocity causes more frictional losses during air pass over heat sink, which is thought to be caused by more turbulence. However, in model 3, which is fully filled with metal foam, the average friction factor increase as a result of using metal foam in the heat sink is around (11, 14, and 17)% with power (14, 22, and 30) W. The differences between friction factor values for the model 2 and model 4 are small, less than 4% at high power 30 W.

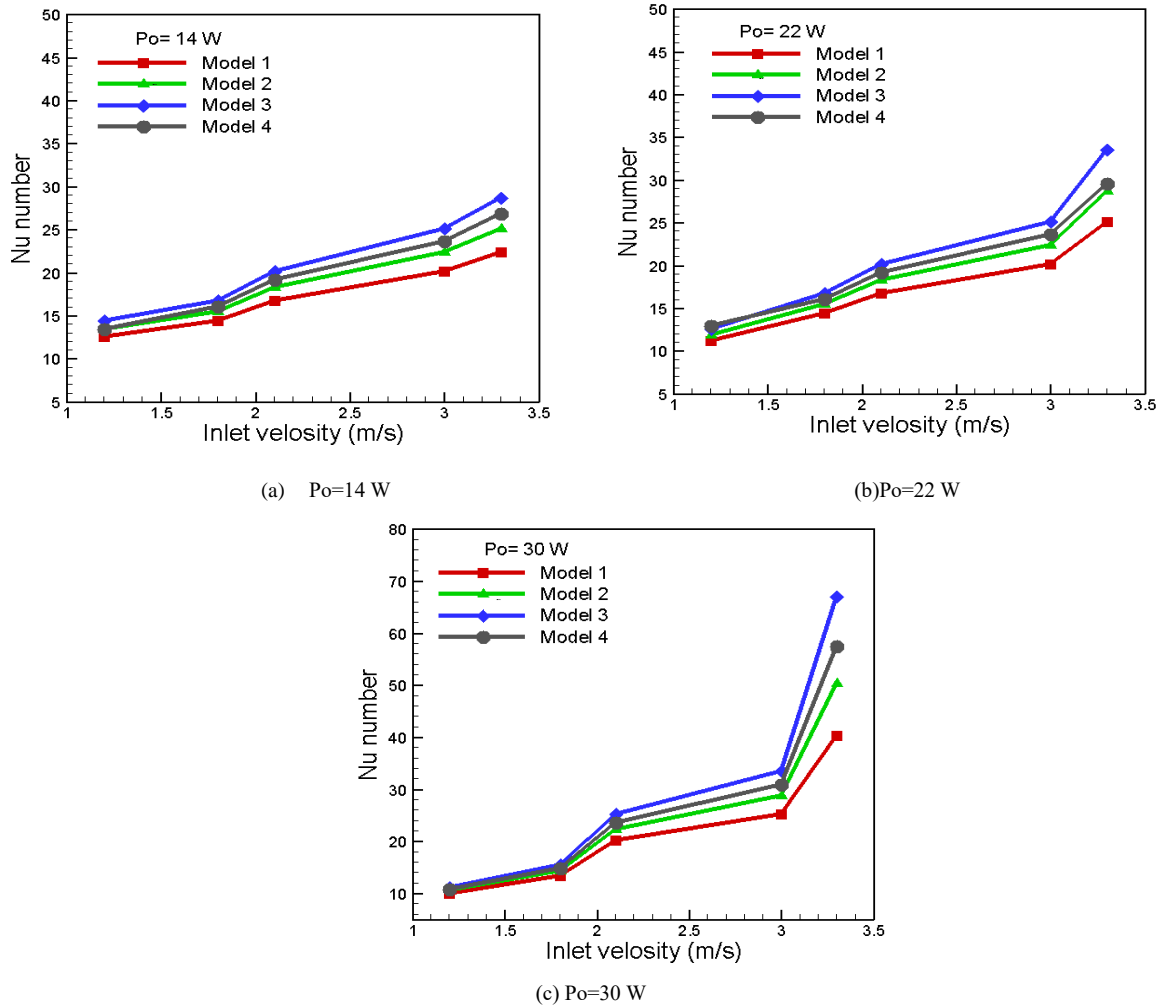


Figure 10. Variation of Nusselt number with inlet velocity at different electric power

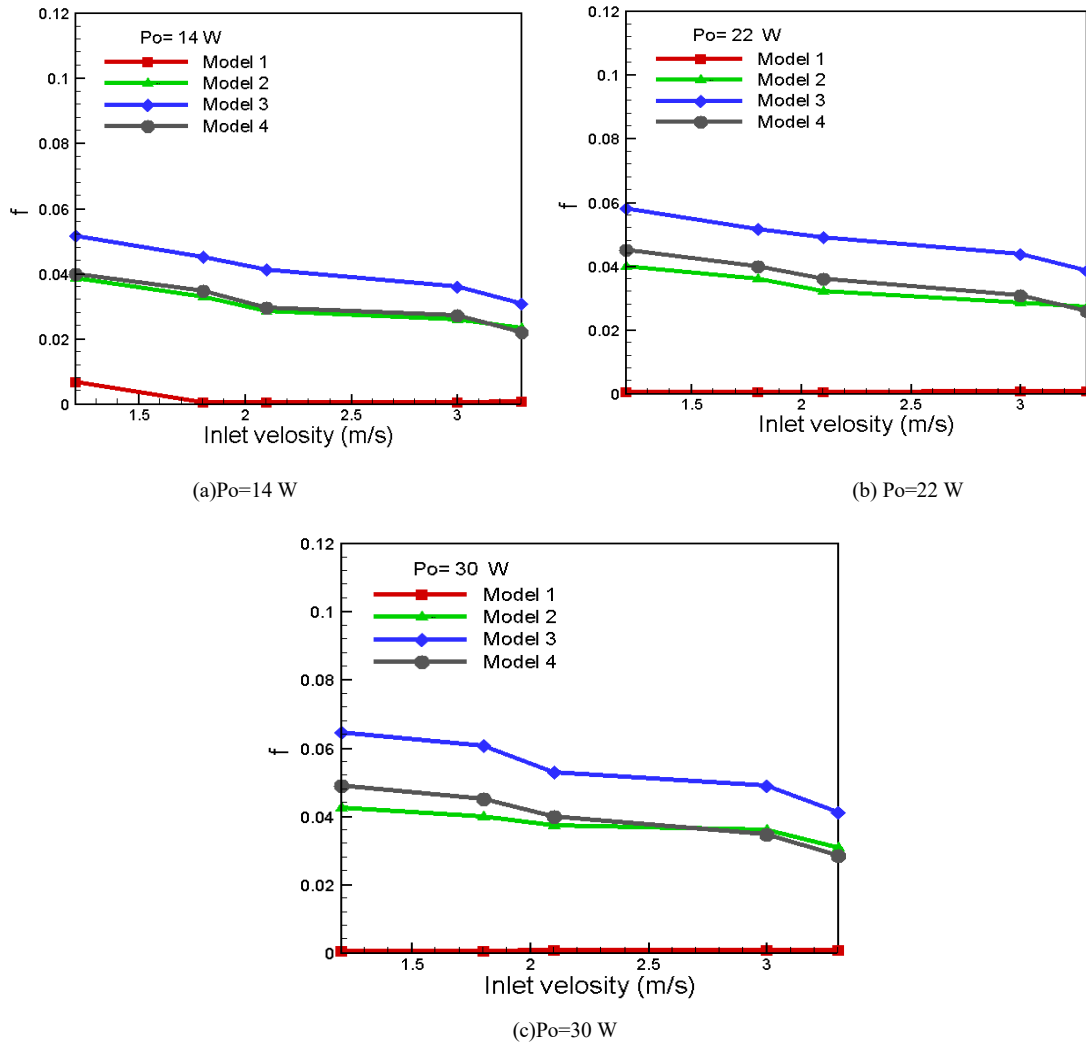


Figure 11. Variation of friction factor with inlet velocity at different electric power

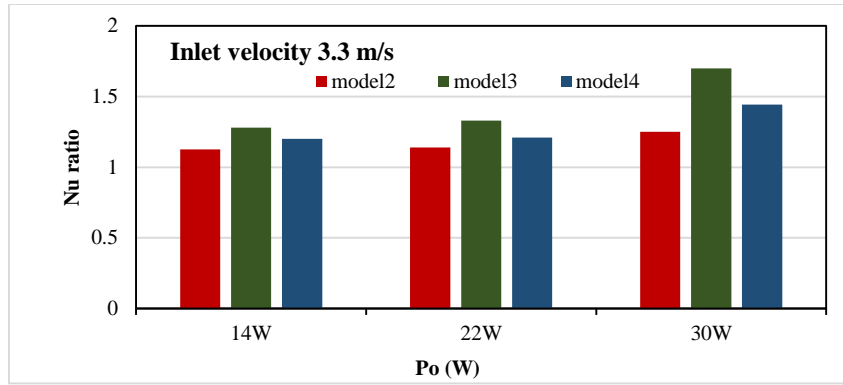
The enhancement ratio of the Nusselt number Nu_{ratio} is an important factor to determine improved heat transfer in the heat sink and can be described as :

$$Nu_{ratio} = \frac{Nu_m}{Nu_{model 1}} \quad (20)$$

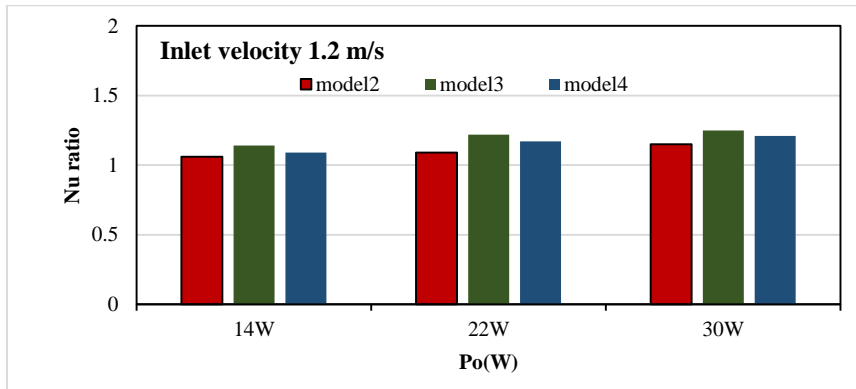
Where Nu_m is the Nusselt number for model 2, 3 or 4.

As illustrated in Fig.12a, model 3 has the better enhancement ratio at high power 30 W; it has improved 6.8% from model 4 and increased 15.7% from model 2 at velocity 3.3 m/s. Also, from Fig.12b can see the model 3 plate foam heat sink significantly performs of the other models of heat sink under a 1.2m/s flow rate, the Nusselt number ratio of model 3 heat sink can be (1.2 -1.46) times of the other models, demonstrating the efficiency of utilizing a metal foam heat sink to cool power electronics.

The thermal resistances for four different models at three different electric power sources and five various inlet velocities are seen in Fig. 13(a, b, and c). Here, the R_{th} was calculated by dividing the temperature difference between the base and surrounding air temperatures by the amount of heat transferred to the heat sink. The heating resistance of heat sinks decreases significantly with increasing inlet air velocity. For all heat flux values, at low rates of flow, the model 1 is higher than the other models for all values of heat flux. However, the model 3 heat sinks exhibit about 22% reduction in thermal resistance at greater flow rates when compared to the model 1 for a power of 30 W. This suggests that the copper foam heat sinks are excellent in performance of cooling. As a result, small cooling systems for electronics could benefit greatly from the use of foam heat sinks.

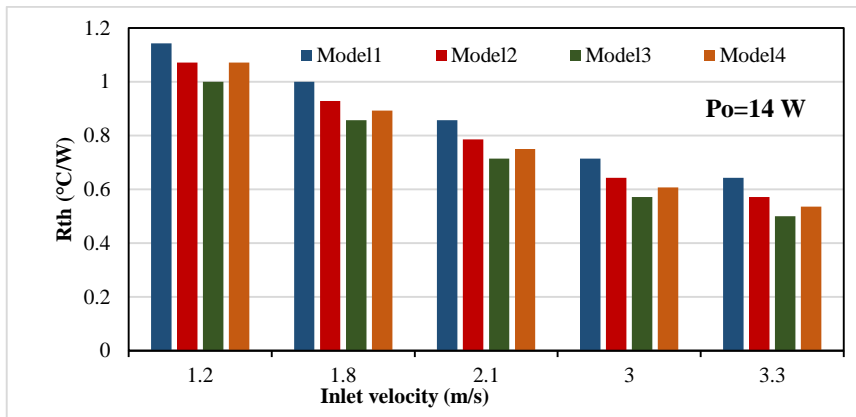


(a) Inlet velocity 3.3 m/s

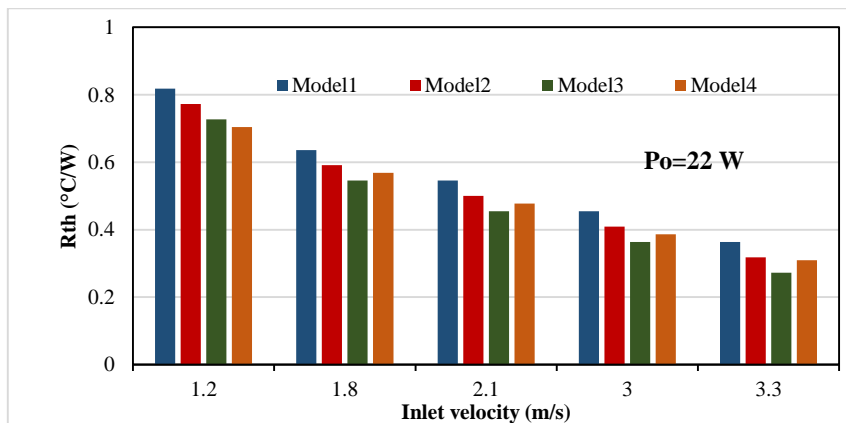


(b) Inlet velocity 1.2 m/s

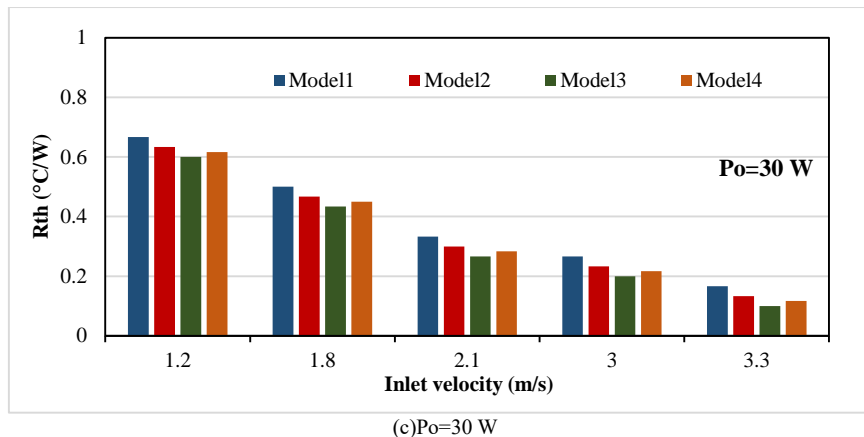
Figure 12. Variation of the Nu ratio for different models of heat sinks



(a) Po=14 W



(b) Po=22 W



(c) $P_o=30$ W
Figure 13. Variation of thermal resistance with inlet velocity for different models

8. Conclusion

The primary aim of this work is to enhance the thermal heat sink design by arranging for of a novel heat sink design involving copper metal foam. The heat sinks were studied with a wide range of Reynolds number, from 2700 and 12000 to evaluate their thermal efficiency. Heat sinks made of metal foam are significantly better in heat dissipation performance than those composed of aluminum. As compared to a conventional heat sink (model 1), heat sinks with metal foam significantly decrease the temperature difference ($T_w - T_a$). It was discovered that the average Nusselt number improved as the Reynolds number increased for all heat sinks. Therefore, a higher Reynolds number will result in a smaller boundary layer, which will improve heat transfer. When comparing the foam plate heat sink (model 3) with traditional fin heat sinks (model 1), the pressure drop is greater for the metal foam model 3, while there is little difference in the pressure drop between models 2 and 4. Furthermore, the improvement in the Nusselt number ratio of the plate foam heat sink is significantly greater than that of the other heat sink models. The use of 40 PPI foam improves the Nu ratio because it increases the amount of internal convection heat transfer region, which allows heat from the bottom wall to diffuse through the whole foam region.

CRedit authorship contribution statement

Sajida Lafta Ghashim: Investigation, Formal analysis, Conceptualization, Methodology, Data curation, Writing - original draft, Writing - Original Draft.

Conflict of interest

The author declared that there is no conflict of interest.

References

- [1] D.S. Steinberg . Cooling techniques for electronic equipment. 2nd edition. Wiley; 1991.
- [2] M. Iyengar , A. Bar-Cohen , " Design for manufacturability of SISE parallel plate forced convection heat sinks", Componenta packaging. Technologies . IEEE Trans., Vol. 24, July 2001, pp. 150–158. <https://doi.org/10.1109/6144.926377>.
- [3] H. Jonsson, B. Palm, "Thermal and hydraulic behavior of plate fin and strip fin heat sinks under varying bypass conditions ". ITherm'98. Sixth Intersociety Conference on Thermal and Thermomechanical Phenomena in Electronic Systems (Cat. No.98CH36208) , 1998. <https://doi.org/10.1109/ITHERM.1998.689525>.
- [4] K. K. Sikka, K. E. Torrance, C. U. Scholler, P. I. Salanova, " Heat sinks with fluted and wavy fins in natural and low-velocity forced convection ". I THERM 2000 .The Seventh Intersociety Conference on Thermal and Thermomechanical Phenomena in Electronic Systems (Cat. No.00CH37069), 2000. <https://doi.org/10.1109/ITHERM.2000.866821>.
- [5] H. Havtun, B.Moshfegh, " Modeling of the thermal and hydraulic performance of plate fin, strip fin, and pin fin heat sinks - Influence of flow bypass". IEEE Transactions on Components and Packaging Technologies, Vol.24 , No.2, 2001, PP.142-149. <https://doi.org/10.1109/6144.926376>.
- [6] K. A. Moores, Y. K. Joshi, G. H.Schiroky, " Thermal characterization of a liquid cooled AlSiC base plate with integral pin fins". IEEE Transactions on Components and Packaging Technologies, Vol.24 , No.2, 2001, PP.213- 219. <https://doi.org/10.1109/6144.926385>.
- [7] M. Saraireh, " Computational fluid dynamics simulation of plate fin and circular pin fin heat sinks", Jordan Journal of Mechanical and Industrial Engineering, Vol.10 , No.2 , June 2016 , PP.99 - 104. <https://jjmie.hu.edu.jo/vol%2010-2/JJMIE-46-15-01.pdf>
- [8] A. Bataineh, W. Batayneh, A. Al-Smadi, B. Bataineh, " Ladder heat sink design using Adaptive Neuro- Fuzzy Inference System (ANFIS)", Jordan Journal of Mechanical and Industrial Engineering, Vol.13, No.3 , May 2019, PP.27- 36. https://jjmie.hu.edu.jo/vol13-1/jjmie_27_19-01.pdf
- [9] H.M. Jaffal, " The effect of fin design on thermal performance of heat sink", Journal of Engineering, Vol.23, No.5, May 2017, PP.123- 146. <https://doi.org/10.31026/j.eng.2017.05.09>.
- [10] M.A. Hussein, " The effect of circular perforation on a V-corrugated fin performance under natural convection", Journal of Engineering, Vol.24, No.7, December 2018, PP.19-34. <https://doi.org/10.31026/j.eng.2018.07>.
- [11] K. A. Jehhef, " Experimental and numerical study effect of using nanofluids in perforated plate fin heat sink for electronics cooling", Journal of Engineering, Vol.24, No.8, July 2018, PP.19-34. <https://doi.org/10.31026/j.eng.2018.08.01>.
- [12] A. S. Salman, M. A. Nima, " Numerical study of fluid flow and heat transfer characteristics in solid and perforated finned heat sinks utilizing a piezoelectric fan", Journal of Engineering, Vol.25, No.7, June 2018, PP.83-103. <https://doi.org/10.31026/j.eng.2019.07.05>
- [13] J. J. Lee, H. J. Kim, D. K. Kim, " Experimental study on forced convection heat transfer from plate-fin heat sinks with partial heating", Processes , Vol.7 , No. 10, 2019. PP. 1-18. <https://doi.org/10.3390/pr7100772>
- [14] R. C. Adhikari, D. H. Wood, M. Pahlevani, " An experimental and numerical study of forced convection heat transfer from

- rectangular fins at low Reynolds numbers", *International Journal of Heat and Mass Transfer*, Vol.163, December 2020. PP. 1-12. <https://doi.org/10.1016/j.ijheatmasstransfer.2020.120418>
- [15] D. Kim, D.K. Kim, " Experimental study of natural convection from vertical cylinders with branched pin fins", *International Journal of Heat and Mass Transfer*, Vol.17, October 2021. <https://doi.org/10.1016/j.ijheatmasstransfer.2021.121545>
- [16] K. Timbs, M. Khatamifar, E. Antunes, W. Lin, "Experimental study on the heat dissipation performance of straight and oblique fin heat sinks made of thermal conductive composite polymers", *Thermal Science and Engineering Progress*, Vol. 22, May 2021, PP. 1-11. <https://doi.org/10.1016/j.tsep.2021.100848>
- [17] S. S. Haghghi, H. R. Goshayeshi, I. Zahmatkesh, " Experimental investigation of forced convection heat transfer for different models of PPFHS heatsinks with different fin-pin spacing", *Heliyon*, Vol. 10, No.1, January 2024, PP.1-14. <https://doi.org/10.1016/j.heliyon.2023.e23373>
- [18] P. C. Huang, K. Vafai, "Analysis of forced convection enhancement in a channel using porous blocks", *Journal of Thermophysics and Heat Transfer*, Vol. 8, No. 3, July 1994, PP. 563- 573. <https://doi.org/10.1016/j.jt.1994.07.003>
- [19] A. Hadim, " Forced convection in a porous channel with localized heat sources", *Journal of Heat Transfer*, Vol. 116, No. 2, May 1994, PP. 465- 47. <https://doi.org/10.1115/1.2911419>
- [20] H. J. Sung, S. Y. Kim, J. M. Hyun, "Forced convection from an isolated heat source in a channel with porous medium", *International Journal of Heat and Fluid Flow*, Vol. 16, No. 6, December 1995, PP. 527- 535. [https://doi.org/10.1016/0142-727X\(95\)00032-L](https://doi.org/10.1016/0142-727X(95)00032-L)
- [21] S. Y. Kim, J. W. Paek, B. H. Kang, "Flow and heat transfer correlations for porous fin in a plate-fin heat exchanger ", *Journal of Heat Transfer*, Vol. 122, No. 3, March 2000, PP. 572- 578. <https://doi.org/10.1115/1.1287170>
- [22] A. K. Shaikdawood, S. S. Mohamed Nazirudeen, " A development of technology for making porous metal foams castings", *Jordan Journal of Mechanical and Industrial Engineering*, Vol. 4, No. 2, March 2010, PP. 292 - 299. https://jjmie.hu.edu.jo/files/v4n2/jjmie-02-09_revised%20modified.pdf
- [23] H. E. Ahmed, I. M. A. Aljbusy, A. A. Farhan, M. Gh. Jehad, " A new microchannel heat sink design using porous media inserts", *Jordan Journal of Mechanical and Industrial Engineering*, Vol. 16, No. 2, March 2022, PP. 225 - 245. <https://jjmie.hu.edu.jo/vol16-2/JJMIE-2022-16-2.pdf>
- [24] S. Feng, F. Li, F. Zhang, T. J. Lu, "Natural convection in metal foam heat sinks with open slots", *Experimental Thermal and Fluid Science*, Vol. 91, February 2018, PP. 354 - 362. <https://doi.org/10.1016/j.expthermflusci.2017.07.010>
- [25] S. Y. Kim; J. W. Paek; B. H. Kang, "Thermal performance of aluminum-foam heat sinks by forced air cooling". *IEEE Transactions on Components and Packaging Technologies*, Vol. 26, No.1, March 2003, PP. 262 - 267. <https://doi.org/10.1109/TCAPT.2003.809540>
- [26] M. A. Alfellag, H. E. Ahmed, M. Gh. Jehad, M. Hameed, "Assessment of heat transfer and pressure drop of metal foam-pin-fin heat sink ", *International Journal of Thermal Sciences*, Vol.170, December 2021, PP.1-15. <https://doi.org/10.1016/j.ijthermalsci.2021.107109>
- [27] A. K. AL-Migdady, A. M. Jawarneh, A. K. Ababneh, H. N. Dalgamoni, " Numerical investigation of the cooling performance of PCM based heat sinks integrated with metal foam insertion ", *Jordan Journal of Mechanical and Industrial Engineering*, Vol.15, No. 2, June 2021, PP. 191 - 197. https://jjmie.hu.edu.jo/vol15-2/04-jjmie_124_20.pdf
- [28] W. E. Akram, S. L. Ghashim, " Investigation of optimum heat flux profile based on the boiling safety factor", *Journal of Engineering*, Vol.25, No. 4, April 2019, PP. 139 - 154. <https://doi.org/10.31026/j.eng.2019.04.10>
- [29] A. I. Zografos, W. A. Martin, J. E. Sunderland, "Equations properties a function of temperature for seven fluids ", *Computer Methods in Applied Mechanics and Engineering*, Vol. 61, No. 2, March 1987, PP. 177-187. [https://doi.org/10.1016/0045-7825\(87\)90003-X](https://doi.org/10.1016/0045-7825(87)90003-X)
- [30] A. Heydari, M. Mesgarpour, M. R. Gharib, "Experimental and numerical study of heat transfer and tensile strength of engineered porous fins to estimate the best porosity", *Jordan Journal of Mechanical and Industrial Engineering*, Vol. 14, No. 3, September 2020, PP. 339-348. <https://jjmie.hu.edu.jo/vol14-3/07-65-20.pdf>
- [31] F. L. Rashid, S. M. Talib, A. K. Hussein, O. Younis, "An experimental investigation of double pipe heat exchanger performance and exergy analysis using air bubble injection technique", *Jordan Journal of Mechanical and Industrial Engineering*, Vol. 16, No. 2, March 2022, PP. 195-204. <https://jjmie.hu.edu.jo/vol16-2/04-84-21.pdf>
- [32] O. Mokhiamar, D. O. Masara, H. El Gamal, " Performance enhancement of multi-modal piezoelectric energy harvesting through parameter optimization ", *Jordan Journal of Mechanical and Industrial Engineering*, Vol. 16, No. 5, December 2022, PP. 677- 688. <https://jjmie.hu.edu.jo/vol16-5/03-JJMIE-157-22.pdf>
- [33] P. Murugesan, K. Mayilsamyb, S. Suresh, " Heat transfer and friction factor in a tube equipped with U-cut twisted tape insert", *Jordan Journal of Mechanical and Industrial Engineering*, Vol. 5, No. 6, December 2011, PP. 559 - 565. <https://jjmie.hu.edu.jo/files/v5n6/JJMIE%20-113-10.pdf>
- [34] J. C. Wang, "Novel thermal resistance network analysis of heat sink with embedded heat pipes", *Jordan Journal of Mechanical and Industrial Engineering*, Vol. 2, No. 1, March 2008, PP. 23 - 30. <https://jjmie.hu.edu.jo/files/V2/003-v2-1.pdf>
- [35] R. M. K. Ali, S. L. Ghashim, " Thermal performance analysis of heat transfer in pipe by using metal foam", *Jordan Journal of Mechanical and Industrial Engineering*, Vol.17, No.2, June 2023, PP. 205-218. <https://jjmie.hu.edu.jo/vol17/vol17-2/05-JJMIE-142-23.pdf>
- [36] J. P. Holman, *Heat transfer*, Sixth Edit. McGraw-Hill, 1986. https://sv.20file.org/up1/412_0.pdf
- [37] D. A. Nield, A. Bejan, *Convection in Porous Media*. Springer and Business Media, New York, 2006.
- [38] A. ALShqiratea, M. Hammadb, M. Tarawnehc, "Cooling of superheated refrigerants flowing inside mini and micro tubes, study of heat transfer and pressure drop, CO2 case study", *Jordan Journal of Mechanical and Industrial Engineering*, Vol. 6, No. 2, April 2012, PP. 199 - 203. <https://jjmie.hu.edu.jo/files/v6n2/jjmie-246-10.pdf>
- [39] J. P. Holman, *Experimental methods for engineering*. Eight Ed. McGraw-Hill Series in Mechanical Engineering, 2007.